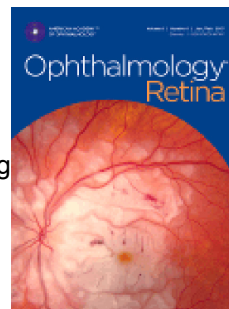


Journal Pre-proof

Detection of macular neovascularization in eyes presenting with macular edema using optical coherence tomography angiography and a deep-learning model

Nida Wongchaisuwat, MD, Jie Wang, PhD, Elizabeth S. White, MS, Thomas S. Hwang, MD, Yali Jia, PhD, Steven T. Bailey, MD



PII: S2468-6530(24)00488-3

DOI: <https://doi.org/10.1016/j.oret.2024.10.017>

Reference: ORET 1835

To appear in: *Ophthalmology Retina*

Received Date: 16 January 2024

Revised Date: 11 October 2024

Accepted Date: 17 October 2024

Please cite this article as: Wongchaisuwat N., Wang J., White E.S, Hwang T.S., Jia Y. & Bailey S.T., Detection of macular neovascularization in eyes presenting with macular edema using optical coherence tomography angiography and a deep-learning model, *Ophthalmology Retina* (2024), doi: <https://doi.org/10.1016/j.oret.2024.10.017>.

This is a PDF file of an article that has undergone enhancements after acceptance, such as the addition of a cover page and metadata, and formatting for readability, but it is not yet the definitive version of record. This version will undergo additional copyediting, typesetting and review before it is published in its final form, but we are providing this version to give early visibility of the article. Please note that, during the production process, errors may be discovered which could affect the content, and all legal disclaimers that apply to the journal pertain.

© 2024 Published by Elsevier Inc. on behalf of American Academy of Ophthalmology

1 Detection of macular neovascularization in eyes presenting
2 with macular edema using optical coherence tomography
3 angiography and a deep-learning model

4 Nida Wongchaisuwat, MD^{1,2}, Jie Wang, PhD¹, Elizabeth S White, MS¹, Thomas S. Hwang, MD¹,
5 Yali Jia, PhD¹, Steven T. Bailey, MD¹

6

7

8 ¹*Casey Eye Institute, Department of Ophthalmology, Oregon Health & Science University, Portland,*
9 *Oregon, USA*

10 ²*Department of Ophthalmology, Faculty of Medicine Siriraj Hospital, Mahidol University, Bangkok,*
11 *Thailand*

12

13

14

15

16

17

18 * Correspondence to:

19

20 Steven Bailey, M.D.

21 Professor of Ophthalmology

22 Casey Eye Institute, Department of Ophthalmology

23 Oregon Health & Science University

24 5115 SW Campus Drive

25 Portland, OR 97239

26 Email: bailstev@ohsu.edu

27 Phone: 503-418-8065

28

29

30

31

32

33

34

35 **Financial support:**

36 This work was supported by the National Institute of Health (R01 EY035410, R01 EY027833, R01
37 EY024544, R01 EY031394, T32 EY023211, UL1TR002369, P30 EY010572); the Jennie P. Weeks
38 Endowed Fund, the Malcolm M. Marquis, MD Endowed Fund for Innovation; an Unrestricted
39 Departmental Funding Grant and Dr. H. James and Carole Free Catalyst Award from Research to
40 Prevent Blindness (NewYork, NY), Edward N. & Della L. Thome Memorial Foundation Award,
41 and the Bright Focus Foundation (G2020168, M20230081). The funding organization had no
42 role in the design or conduct of this research.

43

44 **Conflict of Interest:**

45 Jie Wang: Optovue/Visionix, Inc (P, R), Genentech, Inc (P,R); Yali Jia: Optovue/Visionix, Inc. (P,
46 R), Optos, plc (P), Genentech, Inc (P, R,F). These potential conflicts of interest have been
47 reviewed and managed by OHSU. Other authors declare no conflicts of interest related to this
48 article.

49

50

51 **Running head:** AI with OCT/OCTA for MNV detection in eyes macular edema

52

53 **Precis:**

54 Artificial intelligence applied to optical coherence tomography (OCT) and OCT angiography can
55 accurately diagnose and segment MNV in eyes with exudative AMD compared to a control
56 group of eyes with presenting with macular edema.

57

58

59

60

61

62

63

64

65

66 **Abstract**

67 Purpose: To test the diagnostic performance of an artificial intelligence algorithm for detecting
68 and segmenting macular neovascularization (MNV) with optical coherence tomography (OCT)
69 and OCT angiography(OCTA) in eyes with macular edema from various diagnoses.

70 Design: Prospective cross-sectional study.

71 Participants: Study participants with macular edema due to either treatment-naïve exudative
72 age-related macular degeneration (AMD), diabetic macular edema (DME), or retinal vein
73 occlusion (RVO).

74 Methods: Study participants were imaged with macular 3x3-mm and 6x6-mm spectral-domain
75 OCTA. Eyes with exudative AMD were required to have MNV in the central 3x3-mm area. A
76 previously developed hybrid multi-task convolutional neural network for MNV detection
77 (aiMNV) and segmentation was applied to all images, regardless of image quality.

78 Main Outcome Measures: Sensitivity, specificity, positive predictive value (PPV), and negative
79 predictive value (NPV) of detecting MNV; and intersection over union(IoU) score and F1 score
80 for segmentation.

81 Results: Of 114 eyes from 112 study participants, 56 eyes had MNV due to exudative AMD and
82 58 eyes with macular edema due to either DME or RVO. 3x3-mm OCTA scans with aiMNV
83 detected MNV with 96.4% sensitivity, 98.3% specificity, 98.2% PPV, and 96.6% NPV. For
84 segmentation, the average IoU score was 0.947 and the F1 score was 0.973. 6x6-mm scans
85 performed well; however, sensitivity for MNV detection was lower than 3x3-mm scans due to
86 lower scan sampling density.

87 Conclusion: This novel aiMNV algorithm can accurately detect and segment MNV in eyes with
88 exudative AMD from a control group of eyes that present with macular edema from either DME
89 or RVO. Higher scan sampling density improved the aiMNV sensitivity for MNV detection.

90

91

92

93

94 Keywords: artificial intelligence; choroidal neovascularization; CNV; macular neovascularization;
95 MNV; OCT angiography

96

97

98

99 **Introduction**

100 Age-related macular degeneration (AMD) is a leading cause of irreversible blindness worldwide.
 101 [1-3] It was classified into non-neovascular AMD and neovascular AMD, characterized by the
 102 development of macular neovascularization (MNV). Exudative AMD develops when MNV
 103 results in hemorrhage, lipid exudation, subretinal fluid (SRF), intra-retinal fluid (IRF), and
 104 fibrosis. Early detection of MNV is critical, as the visual outcome of MNV treatment is better
 105 when diagnosed early. [4, 5]

106 While fluorescein angiography (FA) has been considered the gold standard for MNV diagnosis,
 107 OCTA has recently become more widely adopted for this purpose, as it generates a detailed
 108 three-dimensional images of the macula and avoids the need for intravenous injection and
 109 relatively long image acquisition time. [6-9] A meta-analysis found that compared to the gold
 110 standard for MNV detection, OCTA performs very well, with an average sensitivity of 0.87 and a
 111 specificity of 0.97. [10] Recent OCTA software enhancements, including the reduction of
 112 motion artifacts and projection artifacts have led to enhanced MNV detection. Because
 113 detection of MNV on *en face* OCTA is dependent on the slab used, improved semi-automated
 114 correction of segmentation errors is useful. [11, 12] An additional advancement is the
 115 application of deep-learning algorithms to automate the detection of MNV with OCTA. [13]

116 Our previous study of MNV diagnosis by human graders concluded that combined *en face* OCTA
 117 with cross-sectional OCT/OCTA images has better sensitivity and specificity for MNV detection,
 118 compared to *en face* OCTA alone. [14] We recently developed an artificial intelligence hybrid
 119 multi-task CNN model for MNV (aiMNV) detection and segmentation that utilized both OCTA
 120 and structural OCT data from a single image acquisition. We evaluated this model using normal
 121 and eyes with other retinal diseases as controls and found it highly sensitive and specific for
 122 MNV diagnosis and MNV membrane segmentation. Our testing of the model demonstrated it
 123 to be more accurate for MNV diagnosis and segmentation when *en face* OCTA was combined
 124 with 3-dimensional structural OCT, compared to tests with *en face* OCTA alone or with 3D
 125 structural OCT alone [15].

126 Other studies have demonstrated that OCTA with human graders is highly sensitive and specific
 127 for MNV detection in AMD. However, one limitation of prior studies is that control eyes were
 128 limited to normal eyes or eyes with intermediate AMD as controls. [14, 16, 17]. These eyes lack
 129 subretinal fluid (SRF), intra-retinal fluid (IRF) on structural OCT and it is possible the SRF and IRF
 130 detected with structural 3D OCT is driving the detection of MNV with artificial intelligence (AI)
 131 based detection. Macular edema causes retinal thickness and reflectivity changes that could
 132 impair MNV detection with *en face* OCTA. A key task in the clinical setting is to accurately
 133 detect MNV as the etiology of the IRF or SRF presenting on cross-sectional structural OCT. To
 134 simulate this, we designed this study to test the performance of the aiMNV algorithm to detect
 135 MNV in eyes with treatment naïve neovascular AMD with active exudation compared to a
 136 control group of eyes with macular edema (IRF, SRF or both) from either diabetic macular
 137 edema (DME) or retinal vein occlusions (RVO).

138

139 **Materials and methods**

140 Patients were enrolled after informed consent was obtained in accordance with a protocol
141 approved by the Institutional Review Board at Oregon Health & Science University and adhering
142 to the tenets of the Declaration of Helsinki. Study participants were recruited from the Retina
143 clinic at the Casey Eye Institute from January 2015 through December 2022.

144 The study is a cross-sectional study with only one visit. The inclusion criteria for enrollment with
145 treatment naïve exudative AMD required age greater than 50 years, drusen, and presence of
146 IRF and/or SRF. MNV was confirmed based on clinical exam and spectral-domain OCT
147 (Spectralis; Heidelberg Engineering, Heidelberg, Germany). MNV was required to be within a
148 3x3-mm area centered on the fovea. All cases were reviewed, and the diagnosis was confirmed
149 by expert retina specialists (STB, NW). In uncertain cases, if FA was available, it was used to
150 confirm MNV. These cases were considered true positives for sensitivity and specificity testing.
151 Inclusion criteria for the control group required eyes to have macular edema (IRF, SRF or both)
152 due to either RVO or DME. The RVO group required the presence of IRF and/or SRF associated
153 with either branch retinal vein occlusion or central retinal vein occlusion based on clinical exam
154 and OCT. The presence of macular edema due to DME required the presence of diabetic
155 retinopathy and IRF and/or SRF based on clinical exam and OCT. Exclusion criteria included
156 MNV outside the 3x3-mm scanning area, macular edema from other diseases than DME and
157 RVO, and MNV due to clinical diagnoses other than AMD.

158 Study participants were scanned with spectral-domain OCTA with either the Avanti RTVue-XR
159 (Visionix/Optovue Inc., Freemont, CA) with center wavelength of 840-nm and 70-kHz scanning
160 rate or the Solix (Visionix/Optovue Inc., Freemont, CA) with center wavelength of 840-nm and
161 120-kHz scanning rate. All study participants had both 3x3-mm and 6x6-mm OCTA scan
162 patterns. In both Avanti and Solix OCTA systems, two consecutive B-scans were acquired at the
163 same location, and the split-spectrum amplitude-decorrelation angiography (SSADA) algorithm
164 was applied to evaluate the flow signals.[18, 19] One X-fast and one Y-fast were acquired and
165 registered for suppressing the motion artifacts.[20] Retinal layers of the inner limiting
166 membrane (ILM), the outer border of the outer plexiform layer (OPL), and Bruch's membrane
167 (BM) were automatically segmented using our customer-designed COOL-ART software.[21]
168 MNV was detected in the *en face* outer retinal slab: between the outer border of OPL and BM.
169 Segmentation errors were corrected using the manual correction implemented in the same
170 software for challenging scans. In order to clearly visualize the MNV vasculature in the outer
171 retina angiogram, projection artifacts in the original OCTA were eliminated using the
172 projection-resolved (PR)-OCTA algorithm.[22]

173 We developed a hybrid multitask CNN model for MNV diagnosis and membrane segmentation
174 (aiMNV). The model was trained using a large real-world dataset consisting of various retinal
175 diseases acquired from five eye clinics.[15] None of the eyes tested in this study were present

176 in the original training database. The inputs of the AI model include both OCT/OCTA volumes
 177 and their 2D projections. For the 2D input component, our algorithm incorporates four *en face*
 178 angiograms from the following OCTA inputs: (1) uncorrected inner retinal angiogram, (2)
 179 uncorrected outer retinal angiogram, (3) slab-subtracted outer retinal angiogram, and (4)
 180 projection-resolved outer retinal angiogram. Both slab subtraction and PR-OCTA are processing
 181 techniques employed to eliminate projection artifacts. [13] Although the projection-resolved
 182 outer retinal angiogram offers a clear MNV vascular pattern, residual projection artifacts may
 183 still be mistaken for the actual MNV signal. Additionally, our network incorporates 2D structural
 184 OCT projections and thickness information for the 2D subnet. Structural images aid in
 185 identifying MNV lesions, as pathologic changes in reflectivity are associated with MNV. To
 186 retain depth information for the network to learn, we partition the structural volume into 10
 187 equal sections, using mean projection to obtain *en face* images. Mean projection images of the
 188 entire structural volume and inner retina are also included. Input from *en face* OCT images and
 189 thickness maps help identify changes in outer retinal thickness and RPE reflectivity associated
 190 with MNV. Additionally, thickness maps for both the inner and outer retina assist in identifying
 191 MNV lesions and recognizing projection artifacts, as they often coincide with retinal pigment
 192 epithelium elevations. The 3D input component incorporates outer retinal structural OCT and
 193 PR-OCTA.

194 We applied a consistent definition for segmenting the MNV. To generate artifact-free outer
 195 retina images displaying clear MNV vasculature, we followed these steps: (1) Utilized the PR-
 196 OCTA algorithm to remove projection artifacts, (2) Segmented the Inner Limiting Membrane
 197 (ILM), Outer Plexiform Layer (OPL), and Bruch's Membrane (BM) layers, (3) segmented the MNV
 198 membrane area using our well trained AI model, (4) applied adaptive thresholding algorithm to
 199 binarize the MNV and remove background noise, (5) displayed only the MNV vessels within the
 200 outer retina. The CNN architecture was designed for the specific purposes of MNV diagnosis
 201 and membrane segmentation, which includes a 2D and 3D subnet for features extraction and
 202 merging, a Res-net-like subnet for MNV diagnosis, and a U-net-like subnet for MNV membrane
 203 segmentation.

204 To assess the performance of the artificial intelligence algorithm, sensitivity, specificity, PPV,
 205 NPV, F1 score, and the Jaccard index for 6x6 and 3x3 scan patterns. SPSS (IBM, SPSS Inc) was
 206 used for statistical analysis. For cases in which both eyes were enrolled from a study
 207 participant, a second analysis was completed after randomly selecting one of the two eyes. All
 208 images of participants in this study have never been used for model training in the previous
 209 study.

210 Results

211 There were 120 eyes from 118 patients enrolled in this study. 58% of the eyes were scanned
 212 with the Solix and 42% with the AvantiRTVue-XR (Visionix/Optovue Inc., Freemont, CA). Two
 213 eyes were excluded due to MNV outside the 3x3-mm scanning zone and 4 eyes were excluded

214 because of incorrect diagnosis. Of the remaining 114 eyes, 56 eyes had treatment naïve
 215 exudative neovascular AMD including type 1, type 2 and type 3 MNV, and 58 eyes had macular
 216 edema due to either RVO or DME. FA was performed in 36 out of 56 cases to confirm the
 217 diagnosis of MNV.

218 The aiMNV algorithm performed better for 3x3 mm scans than 6x6 mm scans (Table 1). Using
 219 the 3x3-mm scan pattern, of 56 true positive MNV eyes, 54 of them were accurately diagnosed
 220 with a sensitivity of 96.4%. Of 58 eyes with macular edema without MNV, 57 were accurately
 221 diagnosed with a specificity of 98.3%. Using the 6x6 mm scan pattern, 46 of 56 true positive
 222 MNV eyes were correctly diagnosed with a sensitivity of 82.1%. Of 57 eyes with macular edema
 223 and no MNV, 54 were correctly diagnosed with a specificity of 94.7% (Table 1). Two subjects
 224 had MNV in each eye, and to assess the potential effects of repeat measurements, an analysis
 225 was repeated using only one eye randomly selected. The repeat analysis demonstrated the
 226 statistics were changed by no greater than 0.4% for 6x6 mm analysis and no greater than 0.2%
 227 for 3x3mm analysis.

228 Of the 54 eyes with MNV detected with the aiMNV algorithm with the 3x3 mm scan, an
 229 automated quantitative measurement of MNV membrane area (Figure 1) was generated in 51
 230 eyes (94%). The average intersection over union (IoU) was 0.947, and the average F1 score was
 231 0.973. The mean MNV membrane area was 1.73 mm² (range = 0.11 - 8.15 mm²).

232 Of those eyes scanned with 3x3 mm scan pattern, two eyes were classified as false negative.
 233 One false negative was associated with a small type 3 MNV (Figure 2). The second false
 234 negative was associated with a large subretinal hemorrhage (SRH) (Figure 3 – Case 4). The lone
 235 false positive case was a study participant with DME as well as intermediate AMD.

236 Fourteen out of fifty-six eyes (25%) in the MNV group had SRH in the macular area. Of these 14
 237 eyes, 10 had only a small area of hemorrhage that did not affect the imaging, while the
 238 remaining 4 had a large area of SRH that obscured the OCTA image. Despite the SRH, the aiMNV
 239 algorithm identified MNV in 3 of these 4 cases. (Figure 3). MNV segmentation was limited to 2
 240 of the 4 cases.

241 Discussion

242 In this study, our aiMNV model demonstrated high performance for MNV diagnosis and
 243 segmentation. One advantage of the aiMNV model is that the algorithm combines 3D structural
 244 OCT and *en face* OCTA simultaneously to improve accuracy of MNV detection. There are several
 245 other studies that have applied deep learning algorithms combining OCT and OCTA to diagnose
 246 MNV. Thakoor et al. reported deep learning model combining OCT and OCTA images for
 247 neovascular AMD detection, and their model demonstrated a lower sensitivity and specificity
 248 than our study, 0.69, 0.82 respectively, along with a F1 score was 0.64. [23] Jin et al. also
 249 developed deep learning model with a novel feature-level fusion method that combines the OCT
 250 and OCTA data for assessing MNV. Their model achieved a high accuracy of 95.5% and an area
 251 under the curve (AUC) of 0.9796, in contrast to a completely healthy group. [24]

252

253 Our study design is different than the previously mentioned studies in that the control group was
254 required to have macular edema. Clinicians often encounter macular edema as an etiology of
255 vision loss. The presence of SRF or IRF on structural OCT is a frequent reason for referral to retina
256 specialist, often with a concern of MNV as a possible source of the fluid. Because untreated
257 exudative neovascular AMD can lead to permanent vision loss with fibrosis and SRH, it is
258 important to identify the presence of MNV to initiate timely treatment. In addition to the key
259 clinical distinction of detecting MNV, we wanted to test if the presence of IRF and SRF may have
260 interfered with the performance of the aiMNV algorithm. Our aiMNV algorithm was found to be
261 highly reliable in detecting MNV cases among a cohort of control eyes with macular edema due
262 either DME or RVO.

263

264 We found the aiMNV algorithm performance was excellent with 3x3-mm scans; however the
265 performance dropped slightly with 6x6-mm scans (Table 1). The reason for this decline is that
266 the larger scanning areas had a reduced sampling density. In 3x3-mm scans, each OCT/OCTA
267 volume has 304 B-frames providing about 10 $\mu\text{m}/\text{line}$ sampling density. In contrast, 6x6-mm
268 scans the OCT/OCTA volume has the same 304 B-frames and the sampling density is reduced by
269 half with 20 $\mu\text{m}/\text{line}$. This reduced imaging density results in lower resolution over a larger area.
270 A second reason for the difference is that the aiMNV algorithm was trained using more 3x3-mm
271 scans, 7063 total scans compared to 3503 total scans using a 6x6-mm scan pattern. Because of
272 these two reasons, small size MNV or MNV with small vessel diameter might be likely more
273 difficult to detect with the aiMNV using 6x6-mm scanning area. In its current form, a larger
274 scanning area may be useful to detect MNV in the macula periphery, however, at a cost of
275 reduced sensitivity. The sensitivity of MNV detection was reduced with the larger scanning area
276 while the specificity remained similar with both the 3x3 and 6x6-mm scanning areas. This is
277 expected because a less dense scanning area would make it more challenging to detect MNV,
278 however it would not be expected to lead to an increase in false positives. In the future, faster
279 scanning OCTs may allow for dense scan patterns with larger scan areas. Additional studies will
280 be needed to optimize training so MNV detection algorithms trained at a given pixel density can
281 be applied to larger or smaller scanning areas without significant loss of performance.

282

283 Reviewing the false positives and negatives may provide insight for further training to improve
284 our aiMNV algorithm. One false negative was associated with a large SRH. In prior studies
285 evaluating the sensitivity and specificity of MNV detection with OCTA with human grading, the
286 presence of large SRH resulted in false negatives for MNV detection. [14, 25] Large SRH blocks
287 OCT signal limiting the ability to detect blood flow in the outer retinal as MNV with OCTA. In this
288 study in eyes with large SRH, aiMNV successfully detected MNV in 3 out of 4 cases (75%). Large
289 SRH are relatively rare, and it is likely that these cases were not well represented in the aiMNV
290 training. The other false negative was associated with a type 3 MNV (Fig 2). Type 3 MNV often
291 are associated with abnormal vasculature in the deep capillary plexus as well as intra-retinal fluid.

292 [26-28] These features are shared in eyes with DME and macular edema associated with RVO.
293 Additional training with type 3 MNV is needed to improve the aiMNV algorithm's ability to
294 discriminate cases that share imaging features.

295
296 Some limitations of our study include the results are limited to the macular edema from the
297 three main specific diagnoses of MNV, DME, and RVO only. It is unknown how IRF or SRF from
298 other retinal diseases may affect the aiMNV algorithm performance. Additionally, we did not
299 encounter a case with a large amount of SRF that could in theory severely attenuate OCTA
300 signal from MNV and impair the performance of the algorithm. Another limitation is a small
301 number of scans of poor quality required manual correction to ensure proper slab boundaries.
302 However, less than 10% of cases in our study require manual segmentation correction. It is
303 likely next generation faster OCT systems will be less likely to have poor quality scans and
304 automated segmentation software is expected to improve limiting the need for manual
305 correction. In the eyes where the aiMNV algorithm detected MNV, the rate of producing a
306 reliable value for membrane area was 94%. We were unable to automatically calculate
307 membrane area in 6%, which may be caused by several reasons including: poor image quality,
308 small sized MNV, or the degree of SRH; each of which could make it difficult to delineate the
309 area of the MNV. Vali et al. demonstrated OCTA with AI-based algorithm could discriminate
310 choroidal neovascularization (CNV) vascular patterns that are associated with CNV activity [29].
311 Our study did not assess the activity based on MNV vascular patterns. Finally, as mentioned
312 above, the aiMNV performance was optimized with the more dense scanning pattern, limiting
313 its effectiveness to the smaller 3x3-mm field of view. However, next generation OCTA systems
314 will be faster allowing the aiMNV algorithm to utilize high density scans with a more practical
315 field of view for clinical practice.

316 As deep learning based methods become an increasingly available tool to assist clinicians with
317 medical diagnoses, it is important that clinicians are confident these algorithms have been
318 tested in scenarios analogous to clinical practice. This study demonstrated our aiMNV had high
319 diagnostic accuracy and that IRF and SRF did not significantly confound the diagnosis and
320 segmentation MNV. In this study, diagnostic accuracy was excellent despite the fact that we did
321 not exclude eyes with poor image quality. However, the confidence in MNV segmentation was
322 limited in eyes with poor image quality.

323 In order for OCT/OCTA coupled with aiMNV to function as an acceptable screening tool to
324 identify eyes with exudative MNV (MNV with IRF/SRF), further improvements are needed. In
325 this study, the only false positive was in an eye with both intermediate AMD and DME. Further
326 study, and possibly additional model training, is needed to improve the accuracy of our model
327 in eyes with early/intermediate AMD in addition to IRF or SRF from an etiology different from
328 MNV. To reduce the risk of false negatives, additional study is needed for eyes with type 3
329 MNV. A possible future application to determine if aiMNV can help detect MNV in cases where
330 diagnosis is unclear based on traditional multi-model imaging.

331 **Conclusion**

332 The aiMNV algorithm successfully diagnosed and segmented MNV compared to a control group
 333 of eyes that presented with macular edema. Higher density scan patterns resulted in improved
 334 aiMNV performance. These results further support that a single scan that simultaneously
 335 provides *en face* OCTA and 3D structural OCT combined with deep learning can reliably
 336 diagnose MNV in a realistic clinical setting.

337

338 **Reference**

- 339 1. Ferris FL, 3rd, Fine SL, Hyman L: **Age-related macular degeneration and blindness due to**
 340 **neovascular maculopathy.** *Arch Ophthalmol* 1984, **102**(11):1640-1642.
- 341 2. Klein R, Klein BE, Knudtson MD, Meuer SM, Swift M, Gangnon RE: **Fifteen-year cumulative**
 342 **incidence of age-related macular degeneration: the Beaver Dam Eye Study.** *Ophthalmology*
 343 2007, **114**(2):253-262.
- 344 3. Wong WL, Su X, Li X, Cheung CM, Klein R, Cheng CY, Wong TY: **Global prevalence of age-related**
 345 **macular degeneration and disease burden projection for 2020 and 2040: a systematic review**
 346 **and meta-analysis.** *Lancet Glob Health* 2014, **2**(2):e106-116.
- 347 4. Canan H, Sızmaz S, Altan-Yaycıoğlu R, SarıTÜRK C, Yılmaz G: **Visual outcome of intravitreal**
 348 **ranibizumab for exudative age-related macular degeneration: timing and prognosis.** *Clin Interv*
 349 *Aging* 2014, **9**:141-145.
- 350 5. Weingessel B, Hintermayer G, Maca SM, Rauch R, Vecsei-Marlovits PV: **The significance of early**
 351 **treatment of exudative age-related macular degeneration: 12 months' results.** *Wien Klin*
 352 *Wochenschr* 2012, **124**(21-22):750-755.
- 353 6. Gao SS, Jia Y, Zhang M, Su JP, Liu G, Hwang TS, Bailey ST, Huang D: **Optical Coherence**
 354 **Tomography Angiography.** *Invest Ophthalmol Vis Sci* 2016, **57**(9):Oct27-36.
- 355 7. Jia Y, Bailey ST, Wilson DJ, Tan O, Klein ML, Flaxel CJ, Potsaid B, Liu JJ, Lu CD, Kraus MF *et al:*
 356 **Quantitative optical coherence tomography angiography of choroidal neovascularization in**
 357 **age-related macular degeneration.** *Ophthalmology* 2014, **121**(7):1435-1444.
- 358 8. López-Sáez MP, Ordoqui E, Tornero P, Baeza A, Sainza T, Zubeldia JM, Baeza ML: **Fluorescein-**
 359 **induced allergic reaction.** *Ann Allergy Asthma Immunol* 1998, **81**(5):428-430.
- 360 9. Stanga PE, Lim JI, Hamilton P: **Indocyanine green angiography in chorioretinal diseases:**
 361 **indications and interpretation: an evidence-based update.** *Ophthalmology* 2003, **110**(1):15-21;
 362 quiz 22-13.
- 363 10. Wang R, Liang Z, Liu X: **Diagnostic accuracy of optical coherence tomography angiography for**
 364 **choroidal neovascularization: a systematic review and meta-analysis.** *BMC Ophthalmol* 2019,
 365 **19**(1):162.
- 366 11. Hormel TT, Huang D, Jia Y: **Artifacts and artifact removal in optical coherence tomographic**
 367 **angiography.** *Quant Imaging Med Surg* 2021, **11**(3):1120-1133.
- 368 12. Zhang M, Hwang TS, Campbell JP, Bailey ST, Wilson DJ, Huang D, Jia Y: **Projection-resolved**
 369 **optical coherence tomographic angiography.** *Biomed Opt Express* 2016, **7**(3):816-828.
- 370 13. Wang J, Hormel TT, Gao L, Zang P, Guo Y, Wang X, Bailey ST, Jia Y: **Automated diagnosis and**
 371 **segmentation of choroidal neovascularization in OCT angiography using deep learning.** *Biomed*
 372 *Opt Express* 2020, **11**(2):927-944.

- 373 14. Faridi A, Jia Y, Gao SS, Huang D, Bhavsar KV, Wilson DJ, Sill A, Flaxel CJ, Hwang TS, Lauer AK *et al*:
 374 **Sensitivity and Specificity of OCT Angiography to Detect Choroidal Neovascularization.**
 375 *Ophthalmol Retina* 2017, **1**(4):294-303.
- 376 15. Wang J, Hormel TT, Tsuboi K, Wang X, Ding X, Peng X, Huang D, Bailey ST, Jia Y: **Deep Learning**
 377 **for Diagnosing and Segmenting Choroidal Neovascularization in OCT Angiography in a Large**
 378 **Real-World Data Set.** *Transl Vis Sci Technol* 2023, **12**(4):15.
- 379 16. Ahmed D, Stattin M, Graf A, Forster J, Glittenberg C, Krebs I, Ansari-Shahrezaei S: **DETECTION OF**
 380 **TREATMENT-NAIVE CHOROIDAL NEOVASCULARIZATION IN AGE-RELATED MACULAR**
 381 **DEGENERATION BY SWEPT SOURCE OPTICAL COHERENCE TOMOGRAPHY ANGIOGRAPHY.**
 382 *Retina* 2018, **38**(11):2143-2149.
- 383 17. Nikolopoulou E, Lorusso M, Micelli Ferrari L, Cicinelli MV, Bandello F, Querques G, Micelli Ferrari
 384 T: **Optical Coherence Tomography Angiography versus Dye Angiography in Age-Related**
 385 **Macular Degeneration: Sensitivity and Specificity Analysis.** *Biomed Res Int* 2018,
 386 **2018**:6724818.
- 387 18. Jia Y, Tan O, Tokayer J, Potsaid B, Wang Y, Liu JJ, Kraus MF, Subhash H, Fujimoto JG, Hornegger J
 388 *et al*: **Split-spectrum amplitude-decorrelation angiography with optical coherence**
 389 **tomography.** *Opt Express* 2012, **20**(4):4710-4725.
- 390 19. Tokayer J, Jia Y, Dhalla AH, Huang D: **Blood flow velocity quantification using split-spectrum**
 391 **amplitude-decorrelation angiography with optical coherence tomography.** *Biomed Opt Express*
 392 2013, **4**(10):1909-1924.
- 393 20. Kraus MF, Potsaid B, Mayer MA, Bock R, Baumann B, Liu JJ, Hornegger J, Fujimoto JG: **Motion**
 394 **correction in optical coherence tomography volumes on a per A-scan basis using orthogonal**
 395 **scan patterns.** *Biomed Opt Express* 2012, **3**(6):1182-1199.
- 396 21. Zhang M, Wang J, Pechauer AD, Hwang TS, Gao SS, Liu L, Liu L, Bailey ST, Wilson DJ, Huang D *et*
 397 *al*: **Advanced image processing for optical coherence tomographic angiography of macular**
 398 **diseases.** *Biomed Opt Express* 2015, **6**(12):4661-4675.
- 399 22. Wang J, Hormel TT, Bailey ST, Hwang TS, Huang D, Jia Y: **Signal attenuation-compensated**
 400 **projection-resolved OCT angiography.** *Biomed Opt Express* 2023, **14**(5):2040-2054.
- 401 23. Thakoor KA, Yao J, Bordbar D, Moussa O, Lin W, Sajda P, Chen RWS: **A multimodal deep learning**
 402 **system to distinguish late stages of AMD and to compare expert vs. AI ocular biomarkers.** *Sci*
 403 *Rep* 2022, **12**(1):2585.
- 404 24. Jin K, Yan Y, Chen M, Wang J, Pan X, Liu X, Liu M, Lou L, Wang Y, Ye J: **Multimodal deep learning**
 405 **with feature level fusion for identification of choroidal neovascularization activity in age-**
 406 **related macular degeneration.** *Acta Ophthalmol* 2022, **100**(2):e512-e520.
- 407 25. de Carlo TE, Bonini Filho MA, Chin AT, Adhi M, Ferrara D, Baumal CR, Witkin AJ, Reichel E, Duker
 408 JS, Waheed NK: **Spectral-domain optical coherence tomography angiography of choroidal**
 409 **neovascularization.** *Ophthalmology* 2015, **122**(6):1228-1238.
- 410 26. Bhavsar KV, Jia Y, Wang J, Patel RC, Lauer AK, Huang D, Bailey ST: **Projection-resolved optical**
 411 **coherence tomography angiography exhibiting early flow prior to clinically observed retinal**
 412 **angiomatous proliferation.** *Am J Ophthalmol Case Rep* 2017, **8**:53-57.
- 413 27. Freund KB, Ho IV, Barbazetto IA, Koizumi H, Laud K, Ferrara D, Matsumoto Y, Sorenson JA,
 414 Yannuzzi L: **Type 3 neovascularization: the expanded spectrum of retinal angiomatous**
 415 **proliferation.** *Retina* 2008, **28**(2):201-211.
- 416 28. Querques G, Souied EH, Freund KB: **Multimodal imaging of early stage 1 type 3**
 417 **neovascularization with simultaneous eye-tracked spectral-domain optical coherence**
 418 **tomography and high-speed real-time angiography.** *Retina* 2013, **33**(9):1881-1887.

420

421 **Figure legend**

422 Figure 1 : Automated generation of macular neovascularization (MNV) membrane area (MA). A:
423 structural optical coherence tomography (OCT) demonstrating type 1 MNV (A1), late phase
424 fluorescein angiography (FA) demonstrating occult MNV (A2), and combined inner retinal slab
425 (purple vessels) and outer retinal slab (yellow vessels) *en face* optical coherence tomography
426 angiography (OCTA) demonstrating MNV with MA = 0.38 mm². B: Structural OCT showing type
427 2 MNV (B1), early phase FA demonstrating classic MNV (B2), and OCTA revealing MNV with MA
428 = 2.87 mm².

429

430 Figure 2 : Example of a false negative case. A: Color fundus photograph with drusen and
431 pigment changes. B: Mid phase fluorescein angiogram (FA) reveals focal hyperfluorescent area
432 corresponding to MNV (red arrow). C: *En face* optical coherence tomography angiography
433 (OCTA) of the outer retina revealing flow signal corresponding leakage on FA (red circle). D:
434 Cross-sectional OCTA revealing flow signal in the deep capillary plexus spiraling posteriorly to
435 the outer retina (yellow arrow) that corresponds to type 3 MNV present with *en face* OCTA and
436 FA.

437

438 Figure 3 : Case examples of automated detection of macular neovascularization (MNV) in cases
439 with large subretinal hemorrhage (SRH) In cases 1-3, aiMNV detected MNV while no MNV was
440 detected in case 4. Top row: color fundus photographs demonstrating cases of large SRH.
441 Second row: OCT demonstrating structural features associated with SRH. C: *En face* optical
442 coherence tomography MNV segmentation for cases 1 and 2 and no MNV segmentation for
443 cases 3 and 4. Probability of MNV detection by aiMNV (P=1), membrane area (MA).

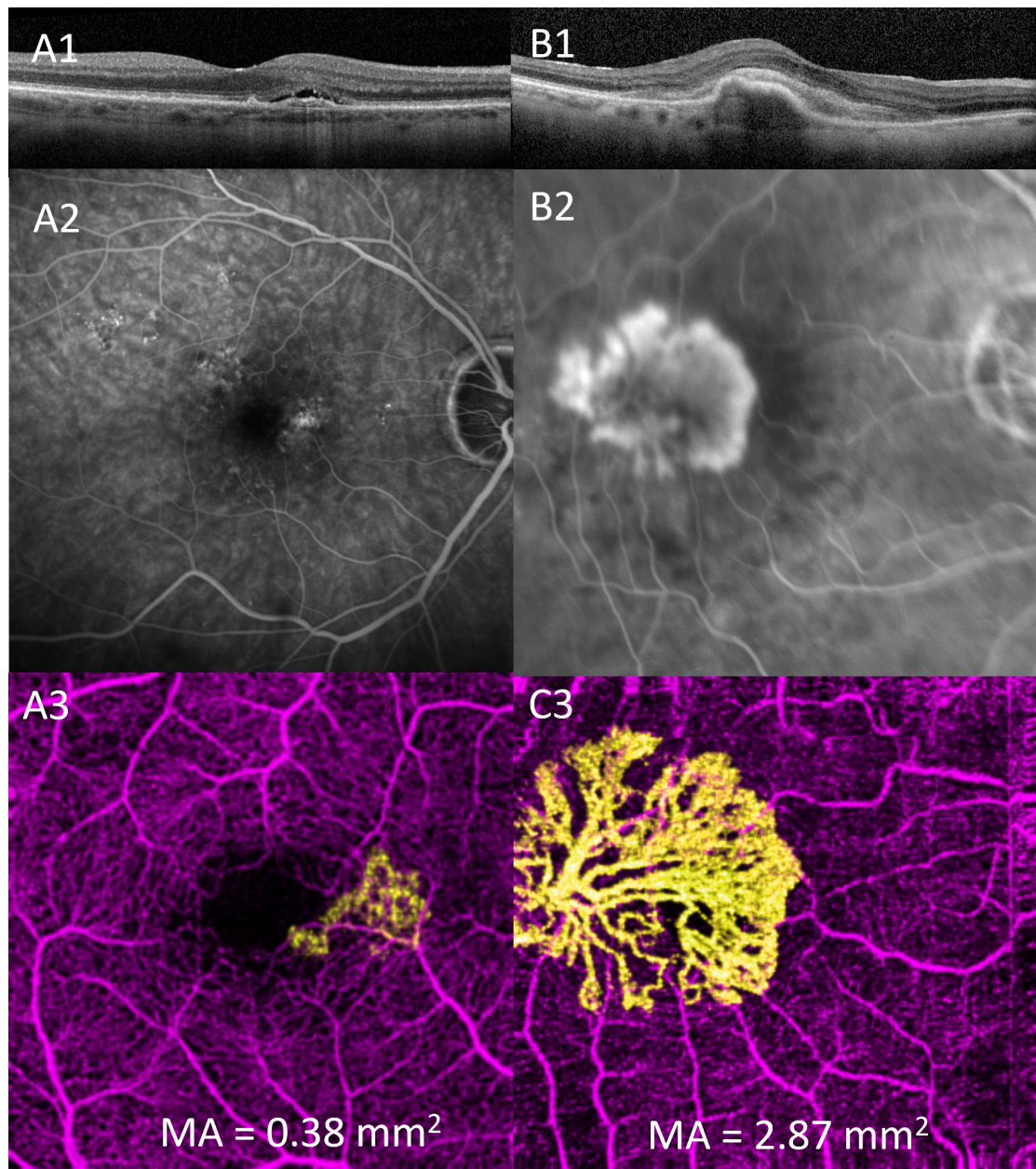
444

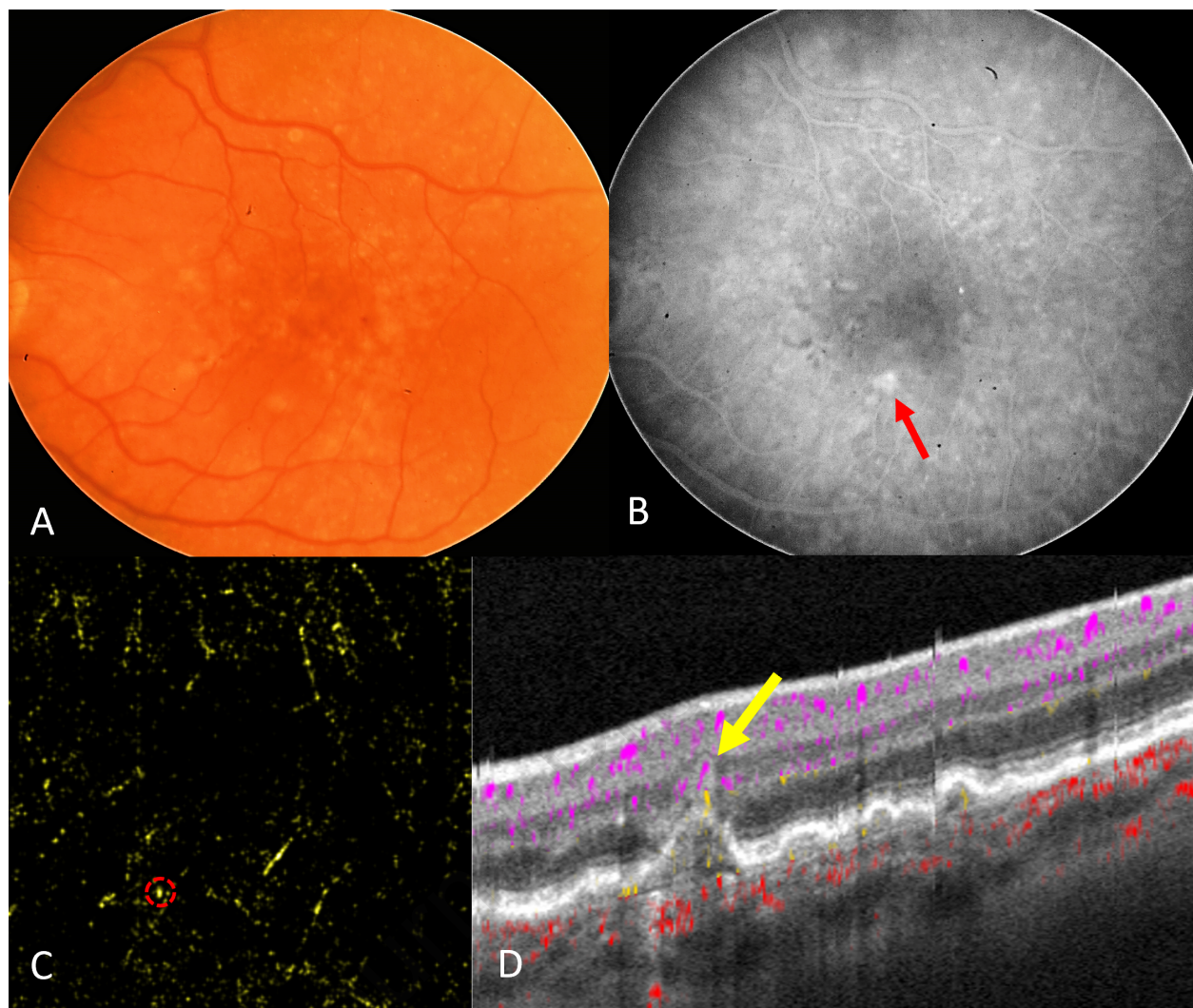
445

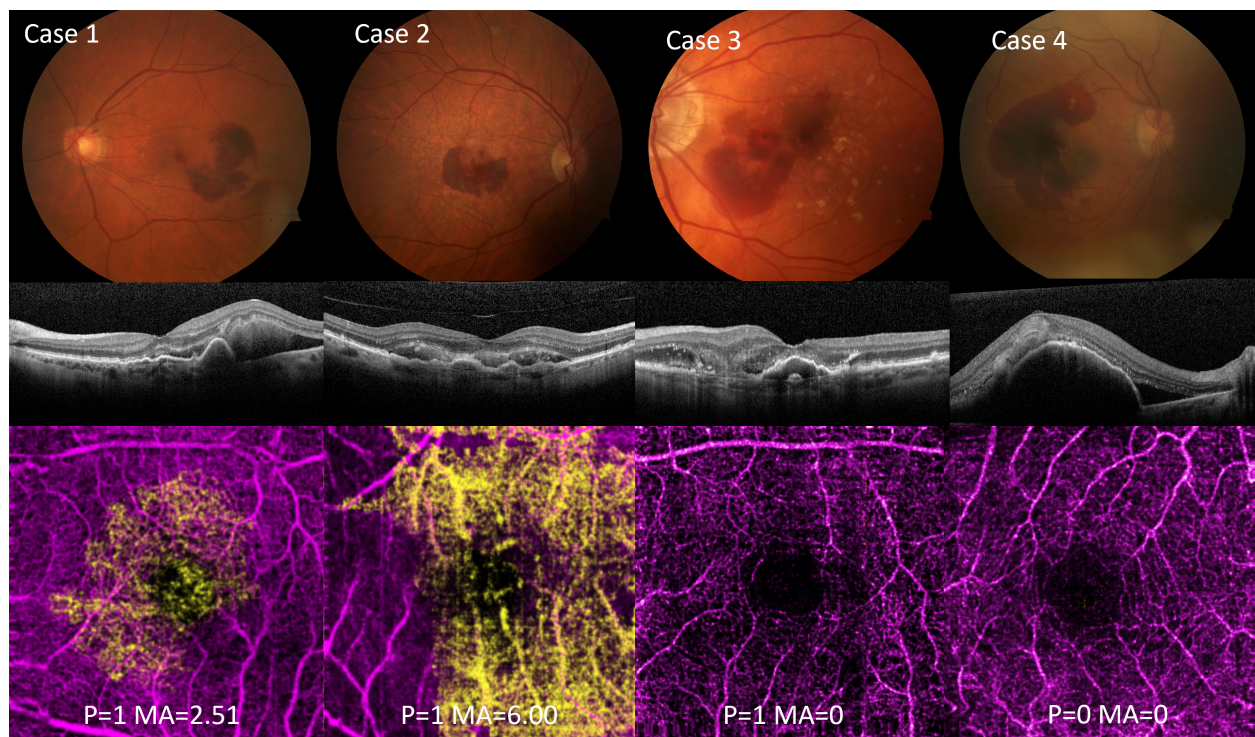
Table 1 The Performance of OCTA with aiMNV Algorithm to Detect and Segment MNV in Eyes with Macular Edema.

	Sensitivity	Specificity	PPV	NPV	F1 Score	IoU
3 x 3 mm - All Eyes	96.40%	98.30%	98.20%	96.60%	0.973	0.947
3 x 3 mm - One Eye per Subject	96.30%	98.30%	98.10%	96.60%	0.972	0.945
6 x 6 mm - All Eyes	82.10%	94.70%	93.90%	84.40%	0.876	0.780
6 x 6 mm - One Eye per Subject	83.30%	94.70%	93.80%	85.70%	0.882	0.789

Abbreviations: ai = Artificial intelligence ; MNV = Macular neovascularization ; PPV = Positive predictive value ; NPV = Negative predictive value ; IoU = Intersection over Union







Precis:

Artificial intelligence applied to optical coherence tomography (OCT) and OCT angiography can accurately diagnose and segment MNV in eyes with exudative AMD compared to a control group of eyes with presenting with macular edema.